Polytechnica (2024) 7 (Suppl 1):1
https://doi.org/10.1007/s41050-023-00042-y

ORIGINAL ARTICLE

Thermal Fatigue of Zircaloy-4 Cladded U-7.5Nb-2.5Zr

Nathanael Wagner Sales Morais[1,2] · Eduardo Franco Monlevade[2] · Cláudio Geraldo Schön[2]

Received: 6 July 2022 / Revised: 16 January 2023 / Accepted: 12 April 2023 / Published online: 21 June 2023

Abstract
Prototype plates made of U-7.5Nb-2.5Zr alloy, also known as Mulberry alloy, cladded with Zircaloy-4 were thermally fatigued between 200 °C and 500 °C investigated. The assembly consisting of a Uranium alloy monolithic core and the Zircaloy-4 cladding was processed by hot rolling and investigated in the "as rolled" state, as well as after applying 9% and 18% reduction in cold rolling. The samples were characterized by Optical microscopy and X-Ray diffraction both before and after the thermal cycling. All samples presented strong volume contraction (shrinkage) in the first thermal cycle, observed concomitantly with the $\gamma \rightarrow \alpha''$ transformation. The relative shrinkage varied with the cold rolling level, being larger for the "as rolled" plate. The failure mechanism observed in all plates was fracture alongside the U-alloy/Zircaloy-4 interface and no transverse crack was observed either in the Zircaloy-4 sheet or in the Uranium core.

Keywords U-7.5Nb-2.5Zr · Thermal fatigue · Phase transformation · Fuel element

1 Introduction

Metallic Uranium alloys are potential candidates to act as fuel elements in research reactors due to their higher density and better thermal conductivity compared with traditional ceramic fuels like UO_2 (Sun et al. 2020; Lopes et al. 2016). The pure metallic Uranium, in spite of showing the highest possible density, presents three allotropic transformations from room to the melting temperature: the base centered orthorhombic phaseα phase, stable at room temperature, the intermediate temperature tetragonal β phase, and the high temperature body centered cubic γ phase. The $\gamma \rightarrow \beta$ phase transformation results in a volume variation (shrinkage) of -0.6%, the $\beta \rightarrow \alpha$phase transformation results in another volume shrinkage of -1%. These phase transformations cause, therefore, dimensional instabilities and accelerates the swelling process, possibly compromising the fuel performance in service (Blackburn 1960; Stobo 1960). The orthorhombicα-U phase shows only four active slip systems, but it deforms also by twinning allowing up to 55% reduction in cold rolling (Lopes et al. 2013). In tensile tests it can can also deform up to 25% elongation, showing therefore some ductility (Cahn 1953; McCabe et al. 2010). Even considering this potential ductility, however, the pureα-U is considered unsuitable for direct application due to the intrinsic anisotropy of the orthorhombic phase.

A traditional solution to this problem is to stabilize the γphase with alloying. Alloying elements like Mo (Burkes et al. 2010; Burkes et al. 2009; Burkes et al. 2009), Nb (Zhang et al. 2010; Zhang 2015; Zhang 2015) and Zr (Basak et al. 2009; Basak et al. 2010; Ghoshal et al. 2014) have been suggested with this intent. In binary alloys, Nb would require a minimum content of 9 wt% in order to the alloy retain theγphase at room temperature after quenching (Justusson 1961), the Zr addition would require circa 50 wt% (Irukuvarghula et al. 2016)and Mo would require circa 7% (Justusson 1961). The addition of these alloying elements may have also positive impact in other properties. Niobium additions, for example, improve the plasticity of theγphase (Ghoshal et al. 2014), and the addition of Zr improves the swelling resistance of the alloy (Ghoshal et al.

✉ Cláudio Geraldo Schön
schoen@usp.br

Nathanael Wagner Sales Morais
nathanaelmorais@gmail.com

Eduardo Franco Monlevade
monlevade@usp.br

[1] Center of Science and Technology of Materials, Instituto de Pesquisas Energéticas e Nucleares - IPEN, Av. Prof. Lineu Prestes, 2242, São Paulo 05508-000, Brazil

[2] Department of Metallurgical and Materials Engineering, Universidade de São Paulo Escola Politécnica, Av. Prof. Mello Moraes, 2463, São Paulo 05508 - 030, Brazil

2014; Takahashi et al. 1989; Leibowitz et al. 1989). Both Nb and Zr together also increase the*solidus*temperature of the U alloys (Ghoshal et al. 2014). Another advantage of using both Nb and Zr is the smaller neutron absorption cross section compared with the Mo (Meyer et al. 2001). The stabilization of theγ phase is, however, not always complete. The addition of Nb and Zr lead to the formation either of the base centered monoclinic α'' or the body centered tetragonal γ^0 metastable transition states (Zhang 2015; Zhang 2015; Volz et al. 2007). The transformation$\gamma \rightarrow \alpha''$results also in shrinkage (Lopes et al. 2013).

In the context of a reactor, the alloy design has to consider also questions related with attaining criticality. It is obvious that the more alloying elements are added, more difficult it is to reach criticality with a given enrichment level. For example, the U – 9Nb – 3Zr was considered inadequate for use as disperse fuel due low U density at 20% enrichment level (Meyer et al. 2001). This fact leads to the search for "optimal" alloys, which have a goodγstability and a suitable U density. One of the "optimal" combinations of the U – Nb – Zr system is the U – 7.5Nb – 2.5Zr alloy, which has good balance between mechanical strength, uranium content, and phase stability (Volz et al. 2007). This alloy is known as Mulberry alloy.

Even with the addition of the alloying elements, the metallic fuel, as in the case of the ceramic base fuels, requires cladding to avoid direct contact with the water of the primary circuit. The commonly used materials for this task are Zr alloys due its higher corrosion resistance and lower cross section for neutron capture (Motta et al. 2015; Kimura et al. 2007; Duan et al. 2017; Baek 2004). Another advantage of Zr alloys is the complete solubility of the Zr in theγ phase of the U, which eases the bonding process during a hot rolling process.

Due to this bonding, the U alloy core and the Zr sheet should resist together the stresses and strains operating during the fabrication and service, in particular, the strains derived of the mechanical constraint. Zircaloy-4, in the hexagonal close packed (HCP) structure, has a linear thermal expansion coefficient (α_T) of about 6×10^{-6} K^{-1} (Materials 2013), the thermal expansion coefficient of the core alloy has not yet been determined, but is surely different. Another important parameter is the*transus* temperature, in which the Zircaloy also presents a temperature dependent phase transformation (HCP $\leftrightarrow$ BCC). This also causes sudden volume changes which can lead to cracks at the bonding layer. This discussion shows that the project of a fuel element which operates around the 250 °C to 350 °C temperature range is complex, since these superposing phase transformations in the core and in the cladding could lead to geometric distortions in operation.

Since most reactor core designs operate at constant temperature, thermal fatigue usually is not of particular concern in the metallic U community. There are instances, however, in which temperature in a reactor can vary (for example, in power transients). The work presented by Lopes et al. (2016) has pointed out that the constraint-driven thermal fatigue of the U – 10Mo/ Zircaloy-4 clad leads to transverse cracks developing across the sheet and the core, a potentially hazardous event, since it could bring the core in contact with the primary coolant circuit in the reactor. Since the U – 7.5Nb – 2.5Zr alloy is suggested as an alternative to the U – 10Mo alloy, a similar investigation of model fuel element plates is required to access its failure mode and the thermal fatigue resistance, which are the aims of the present work.

2 Experimental Procedure

2.1 Sample Preparation

One U – 7.5 Nb – 2.5 Zr alloy slug was Vacuum Induction melted in a carbon crucible using as raw materials natural metallic U ($U^{235} < 0.7\%$, with major impurities: 147 ppm Mn , 95 ppm Ni, 47 ppm Cu, 19ppm Fe and 15ppm O), sponge Zr (major impurities: 0.166 ppm Fe and 0.022 ppm Hf, 2 ppm O) and high purity Nb (major impurities: 0.14 ppm Ta, 0.25 ppm O). The melting procedure is similar to the one reported in the previous works of the group (Morais 2017; Morais 2015; Morais et al. 2018; Morais 2018; Sales 2020). The molten alloy was then cast into a copper mold. The chemical composition of the obtained alloy was determined as U – 7.4 Nb – 2.3 Zr was measured through inductivelly coupled plasma - optical emission spectrometry (ICP-OES). After the casting, the samples were homogenized at1000 °C for 5h in high purity Argon atmosphere, followed by water quenching in order to stabilize the γ phase.

The sample was the hot rolled together with the Zircaloy-4 sheet using the procedure reported by Lopes et al. (2016), in order to fabricate a prototype of co-laminated plate.

2.2 Thermal Cycling

After the hot rolling, the original plate was cut in to two 15 mm x 20 mm x 2 mm pieces. One piece was used as control and designated as HR, the other was cold rolled to 1.82 mm thickness (true strain in the normal direction: $e = -0.094$), then transversely cut in half and named CR9, the other half was cold rolled to 1.64 mm thickness ($e = -0.198$) and named CR18. The cold rolling reduction was carried in a laboratory scale mill using 0.05mm reduction per pass. Since the transverse dimension of the plate did not change significantly, the rolling process can be considered to be performed approximately under plane strain condition.

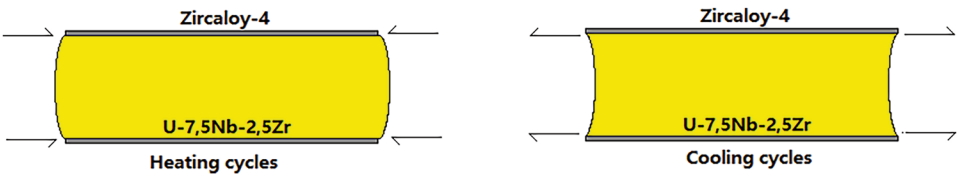

Fig. 1 Expected strains and stresses developed during the heating and cooling cycles in the samples

The HR, CR9 and CR18 samples were cut into 2 x 2 x t (t = thickness) mm^3 pieces in order to fit the thermomechanical analyzer (TMA) instrument *Setaram Multi HTC* (Setaram 20–1600 °C). The cycles were carried in the interval 200° to 500° under high purity Ar atmosphere in a 5 K min^{-1} heating/cooling rate. The actuator of the TMA equipment was placed in contact with the Zircaloy-4 in the normal direction.

Since the sample is a "sandwich" of U alloy inside two zircaloy-4 foils, the constraint acts both in the transversal and in the rolling direction, being accomodated by a shearing stress. Figure 1 shows the expected strain and stresses developed during the thermal cycles. This configuration was chosen because the normal direction is free to expand and to contract during the thermal cycling, which is the displacement measured in the TMA.

2.3 Sample Characterization

The treated samples were cold mounted in polymethyl methacrylate (PMMA) resin for metallographic preparation. Microstructural characterization was performed by Optical Microscopy. Samples were ground with SiC paper and mechanically polished with 1 μm diamond paste. Electropolishing was then carried out using an electrolyte containing 10 % oxalic acid solution in water for 5s using 2 V potential and using stainless steel as the cathode material. The same electrolyte was used for etching using 5 V potential at room temperature.

X-Ray diffraction (XRD) was performed using a PANalytical-Empyrean diffractometer with XCelerator detector. The measurements were performed at room temperature with filtered Cu Kα radiation ($\lambda = 0.15418$ nm) in the $\theta/2\theta$ mode, with 2θrange between 30° to 55°, with a 0.03° step. The U phases were identified using models suggested by Lopes, and Rietveld refined to find a match in the XRD results (Lopes 2013), the Zr phases were identified using the CIF proposed by Wyckoff (1948).

Both phase identification and the peak indexation were performed using the GSAS software based on data available in literature (Toby and Von Dreele 2013).

3 Results and Discussion

Figure 2 shows the initial microstructure and interface of the sample after the hot rolling. The U matrix shows typical γ microstructure with some non-metallic inclusions. No

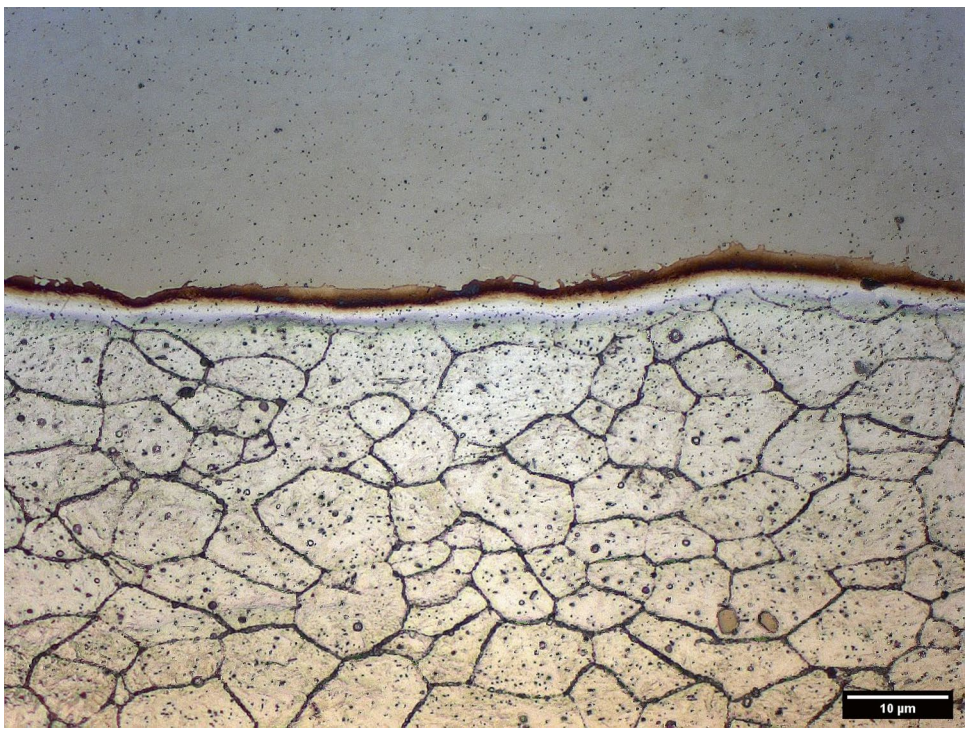

Fig. 2 Initial microstructure of the co-laminated sample

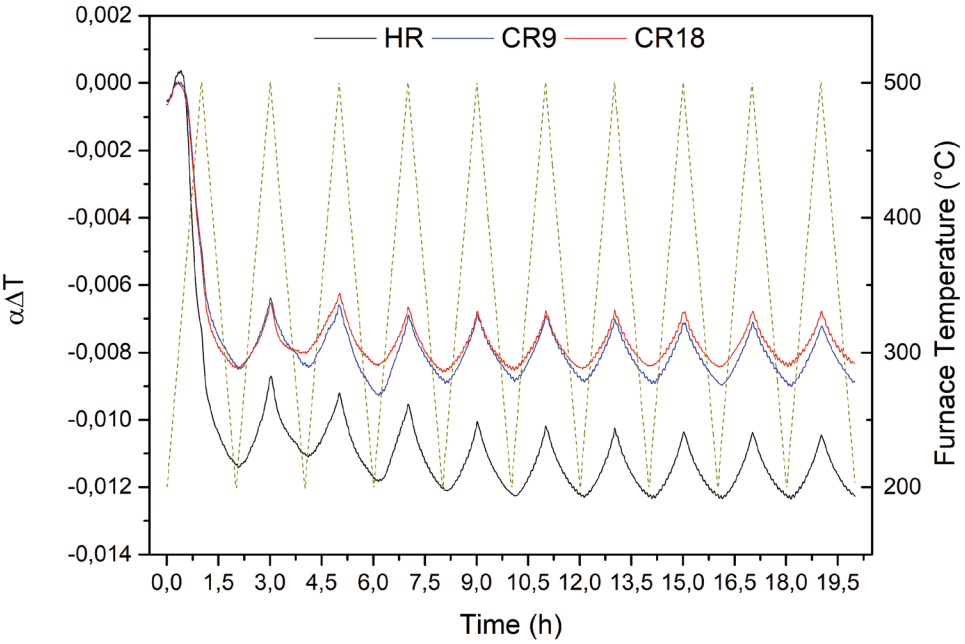

Fig. 3 Relative displacement of samples HR, CR9 and CR18

perceptible cracks were found on the exterior of the sample and also no cracks can be seen on the interface or in the alloy. The cold rolled samples also do not show the presence of fractures on the interface or in the U alloy after the cold rolling. A transition layer between the U and Zr regions can be seen as a light etching constituent. This is a diffusion layer between U and Zr, and very probably β Zr, body centered cubic. The transition from α to β Zr is associated with a 5% expansion. At this point, this volume change does not cause a failure, but further transformation may cause the volume change to become too large to be properly accommodated.

Figure 3 solid lines shows the relative displacement ($\Delta L\ L_0$) for samples HR, CR9 and CR18 and the dashed line presents the furnace temperature in function of time. The first cycle of all samples presents a strong shrinkage at the

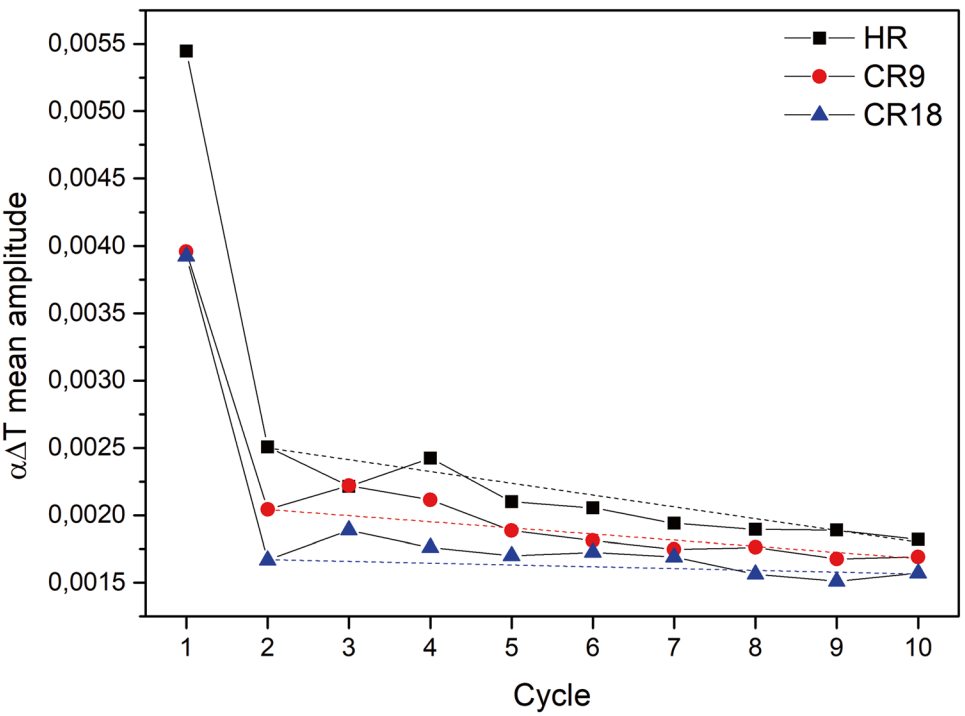

Fig. 4 Maximum amplitude of the relative displacement in each cycle of samples HR, CR9 and CR18

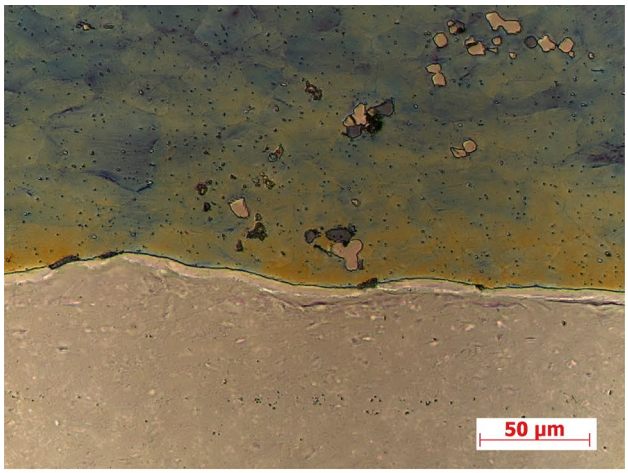

(a)

(b)

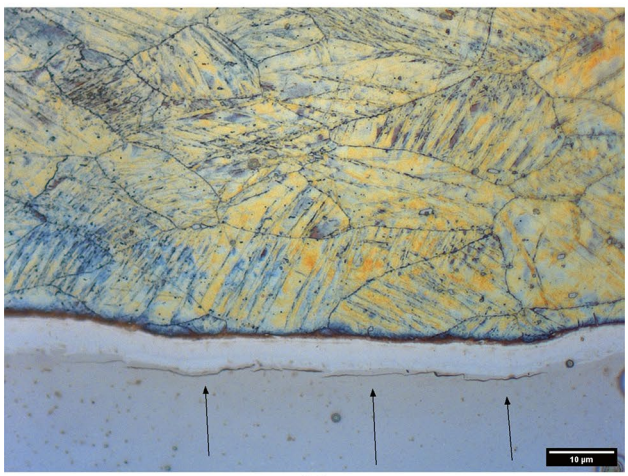

(c)

Fig. 5 Microstructure of the cycled HR (**a**), CR9 (**b**) and CR18 (**c**) plates in the interface between the Zircaloy sheet and the Uranium core

temperature of 330 °C, the HR sample shrinks -1.08%, the CR9 sample presents -0.79% and the CR18 shows -0.78%. The shrinkage is likely caused by the $\gamma \rightarrow \alpha''$ phase transformation, as reported by Lopes et. al. (2013). At the end of the cycling, the HR sample presented a residual strain of -1.17%, the CR9 a residual strain of -0.89% and the CR18 a residual strain of -0.77%. Figure 4 presents the maximum amplitude of the the following cycles. Cycles 2 to 4 presents similar behavior in all samples, increasing the mean amplitude then after cycle 5, all samples presents consistent amplitude reduction.

After the $\gamma \rightarrow \alpha''$ phase transformation, no fast phase transformations are expected in the U – 7.5Nb – 2.5Zr and also in the Zircaloy-4. The reduction on the mean amplitude is therefore not related to any reported phase transformation, therefore it should be related with the reduction of the assembly compliance due to a growing crack.

Figure 5 presents the microstructures of the samples HR, CR9 and CR18 after the thermal cycling. The U grains on all samples present profuse deformation twinning, as the monoclinic structure of U alloys at the rolling temperature has very few slip systems to allow dislocation glide to be a predominant deformation mechanism. All samples presented cracks along the interface of the U – 7.5 Nb – 2.5 Zr alloy, but at the Zircaloy side of the interface. The cold rolling also appears to accelerate the cracking process in the interface, since the cracks on the CR18 sample are larger than the ones in the CR9 sample. The diffusion layer can also be observed in Fig. 4. The cracking occurs parallel to the diffusion layer interface with α Zr, indicating that the cause of the cracking may be strongly linked to volume changes during phase transitions.

The normal direction does not have significant resistance do thermal expansion since both materials are free to expand and shrink without interference. The TMA actuator is placed on the normal direction and its signal is the sum of the thermal expansion of the Zircaloy-4 and the U - 7.5Nb - 2.5Zr.

The bonding between Zircaloy-4 and the U - 7.5Nb - 2.5Zr is the spource of constraint, blocking the expansion or contraction of the U alloy. The cracks nucleate, thus, from a shearing stress due to this constraint. Since there is no constraint in the normal direction, the stresses on the normal direction should initially vanish. Aftertyhe first crack is open, however, the stress state changes such that it accelerates the crack propagation during the heating cycles and delays during the cooling cycles.

Figure 6 shows the XRD patterns for the Initial, HR, CR9 and CR18 samples. The α_{Zr} peaks does not presents significant changes, showing the typical (100), (111) and (012) peaks. The initial sample presents the γ (110) and (200) peaks as expected. The HR, CR9 and CR18 presents the doublet α'' (110)/(021), and no residual γ peaks, as expected due to the $\gamma \rightarrow \alpha''$.

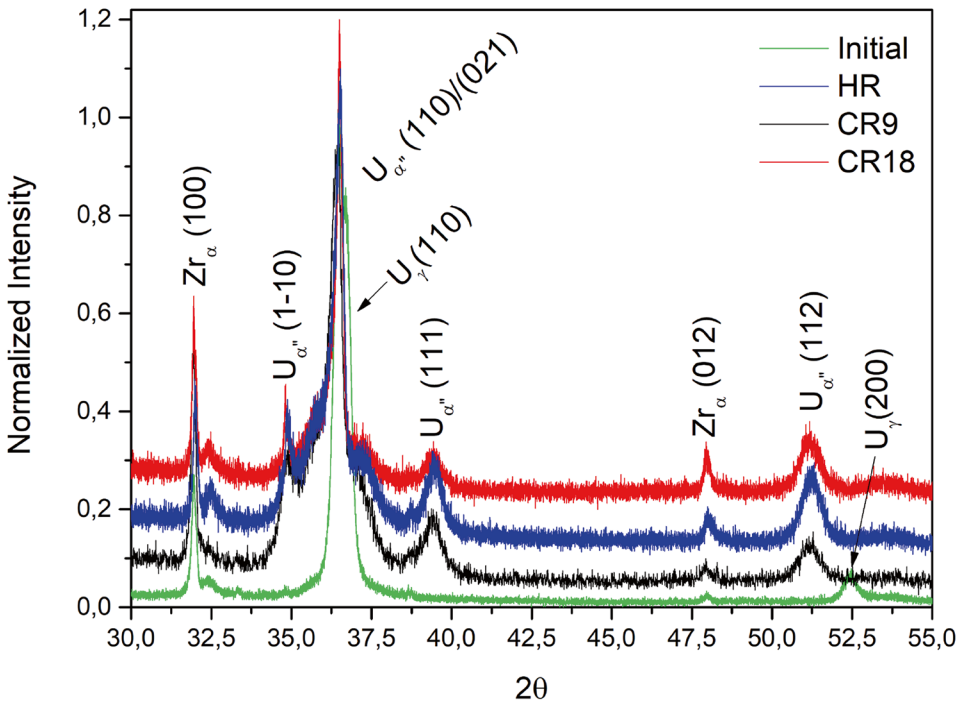

Fig. 6 X-Ray diffraction patterns to Initial, HR, CR9, CR18 samples

4 Conclusions

This work had the objective of evaluate the effect of the thermal fatigue in monolithic metallic U-7.5Nb-2.5Zr fuel elements after hot and cold rolling. The conclusions are:

- The $\gamma \rightarrow \alpha''$ causes strong shrinkage in the normal direction, but this contraction does not implies in fracturing initially.
- Thermal fatigue induces cracking of the interface of the monolithic plates, but always parallel to the interface and inside the Zircaloy sheet, therefore this cracking should not be considered catastrophic, nonetheless further studies are necessary to study the crack propagation.
- Cold rolling has significant effect on the cracking on the interface. The more reduction is performed, the longer are the cracks. Since cold rolling operations are performed in order to straighten the plate and improve surface quality, it should be limited to the least as possible reduction.

Acknowledgements The authors thank Ricardo Gonçalves Gomide and Selma Luíza Silva (CTM-Aramar, Iperó-SP, Brazil) for granting laboratory access and assistance in the experiments. This study was financed in part by the National Science and Technology Development Council (CNPq, Brasília-DF, Brazil) under projects 308565/2018-5 and 307627/2021-7.

Data Availability Data obtained in this research are available from the authors upon request.

References

Baek JH, Park KB, Jeong YH (2004) Oxidation kinetics of zircaloy-4 and zr–1nb–1sn–0.1fe at temperatures of 700–1200 °C. J Nucl Mater 335(3):443–456. https://doi.org/10.1016/j.jnucmat.2004.08.007

Basak C, Prasad GJ, Kamath HS, Prabhu N (2009) An evaluation of the properties of as-cast U rich U - Zr alloys. J Alloys Comp 480:857–862. https://doi.org/10.1016/j.jallcom.2009.02.077

Basak CB, Prabhu N, Krishnan M (2010) On the formation mechanism of the UZr_2 phase. Intermetallics 18:1707–1712. https://doi.org/10.1016/j.intermet.2010.05.006

Blackburn WS (1960) α – β thermal cycling of uranium. J Nucl Mater 2(2):191. https://doi.org/10.1016/0022-3115(60)90049-0

Burkes DE, Prabhakaran R, Jue J-F, Rice FJ (2009) Mechanical properties of DU-xMo alloys with x = 7 to 12 weight percent. Metall Mater Trans A 40:1069–1079. https://doi.org/10.1007/s11661-009-9805-5

Burkes DE, Prabhakaran R, Jue J-F, Rice FJ (2009) Mechanical Properties of DU-xMo Alloys with x = 7 to 12 Weight Percent. Metall and Mater Trans A 40(5):1069–1079. https://doi.org/10.1007/s11661-009-9805-5

Burkes DE, Prabhakaran R, Hartmann T, Jue J-F, Rice FJ (2010) Properties of DU-10wt% Mo alloys subjected to various post-rolling heat treatments. Nucl Eng Des 240:1332–1339. https://doi.org/10.1016/j.nucengdes.2010.02.008

Cahn RW (1953) Plastic deformation of alpha-uranium; twinning and slip. Acta Metall 1(1):49–70. https://doi.org/10.1016/0001-6160(53)90009-1

Duan Z, Yang H, Satoh Y, Murakami K, Kano S, Zhao Z, Shen J, Abe H (2017) Current status of materials development of nuclear fuel cladding tubes for light water reactors. Nucl Eng Des 316:131–150. https://doi.org/10.1016/j.nucengdes.2017.02.031

Ghoshal K, Kaity S, Mishra S, Kumar A (2014) Microstructural investigation of uranium rich U - Zr - Nb ternary alloy system. J Nuclear Mater 446:217–223. https://doi.org/10.1016/j.jnucmat.2013.12.015

Irukuvarghula S, Ahn S, McDeavitt SM (2016) Decomposition of the γ phase in as-cast and quenched u-zr alloys. J Nucl Mater 473:206–217. https://doi.org/10.1016/j.jnucmat.2016.02.028

Justusson WM (1961) Transformation kinetics of gamma-phase uranium molybdenum-niobium alloys. J Nucl Mater 4(1):37–45. https://doi.org/10.1016/0022-3115(61)90147-7

Kimura A, Cho HS, Toda N, Kasada R, Yutani K, Kishimoto H, Iwata N, Ukai S, Fujiwara M (2007) High burnup fuel cladding materials r and d for advanced nuclear systems. J Nucl Sci Technol 44(3):323–328. https://doi.org/10.1080/18811248.2007.9711289

Leibowitz L, Blomquist RA, Pelton AD (1989) Thermodynamics of the uranium-zirconium system. J Nucl Mater 167:76–81. https://doi.org/10.1016/0022-3115(89)90426-1

Lopes DA (2013) Interação entre precipitação e recristalização em liga de urânio contendo niábio e zircônio (Mulberry alloy). https://doi.org/10.11606/T.3.2013.tde-29102014-171203

Lopes DA, Restivo TAG, Padilha AF (2013) Mechanical and thermal behaviour of U - Mo and U - Nb - Zr alloys. J Nuclear Mater 440:304–309. https://doi.org/10.1016/j.jnucmat.2013.05.014

Lopes DA, Zimmermann AJO, Silva SL, Piqueira JRC (2016) Thermal cycling effect in U-10Mo/Zry-4 monolithic nuclear fuel. J Nuclear Mater 473(Supplement C):136–142. https://doi.org/10.1016/j.jnucmat.2016.02.029

Materials A (2013) Zircaloy-4(Alloy Zr4) (UNS R60804) data sheet. https://www.azom.com/article.aspx?ArticleID=7644

McCabe RJ, Capolungo L, Marshall PE, Cady CM, Tomé CN (2010) Deformation of wrought uranium: Experiments and modeling. Acta Mater 58(16):5447–5459. https://doi.org/10.1016/j.actamat.2010.06.021

Meyer MK, Hofman GL, Wiencek TC, Hayes SL, Snelgrove JL (2001) Irradiation behavior of u-nb-zr alloy dispersed in aluminum. J Nucl Mater 299(2):175–179. https://doi.org/10.1016/S0022-3115(01)00676-6

Morais NWS, Lopes DA, Schön CG (2017) Effect of thermo-mechanical processing on microstructure and mechanical properties of U – Nb – Zr alloys: Part 1 - U – 6 wt. % Nb – 6 wt. % Zr. J Nuclear Mater 488:173–180. https://doi.org/10.1016/j.jnucmat.2017.03.006

Morais NWS, Lopes DA, Schön CG (2018) Effect of thermo-mechanical processing on microstructure and mechanical properties of U - Nb - Zr alloys: Part 2 - U - 3 wt % nb - 9 wt % Zr and U - 9 wt% Nb - 3 wt% Zr. J Nuclear Mater 502:51–59. https://doi.org/10.1016/j.jnucmat.2018.01.045

Morais NWS (2018) Influência dos teores de Nb e Zr e do processamento na microestrutura e propriedades mecânicas de ligas U-Nb-Zr. Dr. Sci. Thesis, Universidade de São Paulo Escola Politécnica. https://doi.org/10.11606/T.3.2018.tde-03052018-092214

Morais NWS, Tunes MA, dos Santos VO, Gomide RG, Schon CG (2015) Influence of zr, mo and nb on microstrucutre of ternary uranium alloys. In: Proceedings of 2015 TopFuel Conference Proceedings Poster, TopFuel-2015, European Nuclear Society, Brussels, Belgium

Motta AT, Couet A, Comstock RJ (2015) Corrosion of Zirconium Alloys Used for Nuclear Fuel Cladding. Annu Rev Mater Res 45:311–343. https://doi.org/10.1146/annurev-matsci-070214-020951

Sales Morais NW, Schön CG (2020) Laves phases in the u - mo - zr system. J Alloys Compd 158070. https://doi.org/10.1016/j.jallcom.2020.158070

Stobo JJ (1960) Alpha beta cycling of uranium. J Nucl Mater 2(2):97–109. https://doi.org/10.1016/0022-3115(60)90037-4

Sun K, Dave AJ, Hu L-W, Wilson EH, Phan S, Jaluvka D (2020) Transitional cores and fuel cycle analyses in support of mit reactor low enriched uranium fuel conversion. Progr Nuclear Energy 119:103171. https://doi.org/10.1016/j.pnucene.2019.103171

Takahashi Y, Yamamoto K, Ohsato T, Shimada H, Terai T, Yamawaki M (1989) Heat capacities of uranium-zirconium alloys from 300 to 1100 k. J Nucl Mater 167:147–151. https://doi.org/10.1016/0022-3115(89)90436-4

Toby BH, Von Dreele RB (2013) Gsas-ii: the genesis of a modern open-source all purpose crystallography software package. J Appl Crystallogr 46:544–549

Volz HM, Hackenberg RE, Kelly AM, Hults WL, Lawson AC, Field RD, Teter DF, Thoma DJ (2007) X-ray diffraction analyses of aged U - Nb alloys. J Alloys Comp 444:217–225. https://doi.org/10.1016/j.jallcom.2006.11.089

Wyckoff RWG (1948) Second edition. interscience publishers, New York, New York hexagonal closest packed, hcp, structure. Crystal Structures 1:7–83

Zhang X, Cui YF, Xu GL, Zhu WJ, Liu HS, Yin BY, Jin ZP (2010) Thermodynamic assessment of the U - Mo - Al system. J Nuclear Mater 402:15–24. https://doi.org/10.1016/j.jnucmat.2010.04.018

Zhang Y, Zhang X, Chen X, Weijun G, Wang X (2015) Effect of grain size on phase stability of monoclinic U – Nb alloy during low-temperature aging. J Nuclear Mater 465(Supplement C):167–169. https://doi.org/10.1016/j.jnucmat.2015.05.020

Zhang Y, Wang X, Xu Q, Li Y (2015) X-ray diffraction study of low temperature aging in U – 5.8wt.%Nb. J Nuclear Mater 456(Supplement C):41–45. https://doi.org/10.1016/j.jnucmat.2014.09.004